Available online at www.sciencedirect.com

SCIENCE DIRECT®

Tectonophysics 397 (2005) 167–179

TECTONOPHYSICS

www.elsevier.com/locate/tecto

Linking dynamic elastic parameters to static state of stress: toward an integrated approach to subsurface stress analysis

S. Tiğrek[a,b,*,1], E.C. Slob[a], M.W.P Dillen[a,2], S.A.P.L. Cloetingh[b], J.T. Fokkema[a]

[a]*Section of Applied Geophysics and Petrophysics, Department of Geotechnology, Delft University of Technology, Netherlands*
[b]*Department of Tectonics and Structural Geology, Faculty of Earth and Life Sciences, Vrije Universiteit, Amsterdam, Netherlands*

Received 17 October 2003; accepted 19 October 2004
Available online 5 January 2005

Abstract

Stress is the most important parameter to understand basin dynamics and the evolution of hydrocarbon systems. The state of stress can be quantified by numerical geo-mechanical modelling techniques. These techniques require static elastic parameters of the rocks as input, while tectonic and gravitational forces are given as explicit boundary conditions to compute the local state of stress at different scales. We developed a technique to determine the density and elastic constants at seismic frequencies using full Zoeppritz inversion on angle-dependent seismic reflection data. The dynamic elastic parameters as obtained from seismic data differ from their static equivalents, which are necessary to determine the static state of stress. The dynamic elastic parameters are related to their static equivalents through experimentally obtained relations. In these rock-physics experiments, the static and dynamic elastic parameters are measured simultaneously during different external loading conditions. The experiments used here are all carried out in a tri-axial pressure machine under equal axial stresses. Then pre-stack seismic data analysis in combination with the relation between the static and dynamic elastic parameters, from the rock-physics experiments, provides the input parameters for geo-mechanical modelling.

Keywords: Dynamic elastic parameters; Static state of stress; Subsurface stress analysis

1. Introduction

Changes in the local state of stress along a horizon boundary is important for petroleum-related applications as well as for structural geology and tectonic applications. In basin studies, stresses have been found the most important tectonic factor in the control of basin stratigraphy and fluid flow (Van Balen and Cloetingh, 1993, 1995).

* Corresponding author. Section of Applied Geophysics and Petrophysics, Department of Geotechnology, Delft University of Technology, Netherlands.
E-mail address: s.tigrek@citg.tudelft.nl (S. Tiğrek).
[1] Presently with Shell International Exploration and Production B.V, Rijswijk.
[2] Presently with the NAM, Assen.

0040-1951/$ - see front matter © 2004 Elsevier B.V. All rights reserved.
doi:10.1016/j.tecto.2004.10.008

We have developed a technique to determine the local state of stress in a formation just below a horizon boundary from combining angle-dependent seismic reflection data with rock-physics experiments to link the static and dynamic elastic parameters through the static state of stress (Simmons and Brace, 1965; Cheng and Johnston, 1981; Plona and Cook, 1995). The technique uses full Zoeppritz inversion on seismic reflection data to determine the dynamic elastic parameters and density. These are then combined to experimentally obtained stress-dependent dynamic–static parameter relations to arrive at an image of the local state of stress along a horizon boundary. Our application is to facilitate geo-mechanical modelling, but the results are just well applicable to derive stress information of reservoirs.

In tectonics, geo-mechanical modelling techniques solve a static problem, based on the force equilibrium equation, usually by finite element techniques. The finite element method is the most widely used geo-mechanical modelling technique to quantify the state of stress at different scales (Beekman, 1994), as it can handle complex geometries of structures composed of different materials and subjected to varying boundary conditions. If we consider an elastic earth, the Young's Modulus of elasticity (E), Poisson's ratio (v) and the mass density (ρ) of the rocks are the three main parameters required to solve a tectonic problem by numerical modelling techniques. Local numerical methods usually require explicit boundary conditions to keep the domain of computation small enough to be numerically feasible.

Here, the boundary conditions should mimic regional tectonic forces. Conventionally, the geometry comes from seismic data analysis, the elastic material parameters and density come from logging data and a priori regional geological and tectonic information is used to obtain equivalent boundary forces. Quantitative information on the tectonic forces is not readily available; at best, local stress values can be obtained from logs (Linjordet and Skarpness, 1992). Seismic data after interpretation and depth conversion provide 2D or 3D model geometry. Available logs and cores provide the necessary material parameters. The number of drillings, especially if a basin scale is considered, is usually insufficient. The boreholes are very often infrequently distributed outside the hydrocarbon production zones. Although we have 2D and 3D geometries from seismic data, our material parameters are derived from 1D data sources, irregularly spaced in the 2D/3D input geometries and which are finally extrapolated to fill the whole geometric model.

As an alternative method to provide input material parameters more continuously along the basin target horizons for geo-mechanical modelling, we propose in this paper to analyse seismic data combining different techniques. Amplitude versus offset (AVO) and amplitude versus angle (AVA) analyses are presently routinely used in quantitative seismic data interpretation to establish a relationship between the plane wave reflection amplitudes and dynamic elastic material parameters for hydrocarbon detection and the monitoring of these parameters over production decades for dynamic reservoir characterization (see Castagna et al., 1993; Dey-Sarkar and Svatek, 1993; Landrø et al., 2001).

The true integration of seismic data analysis in geo-mechanical modelling can be achieved by considering that dynamic elastic parameters in small strain experiments are different from the static equivalents and they are related through the static state of stress. Then the quantitative relation between the dynamic and elastic parameters can be used to construct two- dimensional and three-dimensional input models for geo-mechanical computations. This will yield stress estimations with improved accuracy and fewer assumptions.

2. Static and dynamic experiments

The methodology to arrive at a local stress value from each multi-angle seismic reflection data set is based on the hypothesis that the dynamic elastic parameters can be related to their static equivalents through the local state of stress. To validate this hypothesis, a series of experimental results are selected. The experiments include static, quasi-static and dynamic experiments, with a set-up consisting of a tri-axial pressure machine, which is capable of building up computer-controlled forces to a maximum of 3500 kN. The set-up is an open system, which implies no pore pressure is included in the experiments. The effective stress can be manipulated only by changing the applied external stress (Wyllie

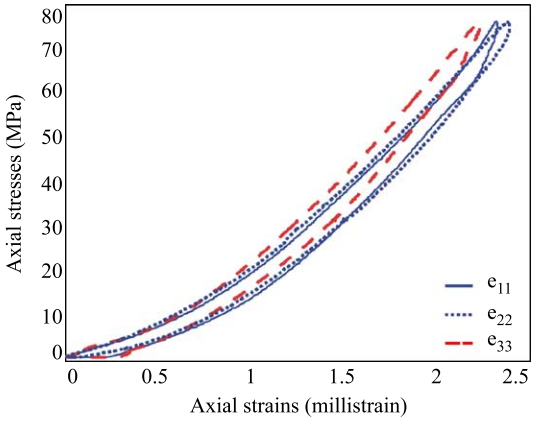

Fig. 1. Flechtinger Sandstone, axial stress (x_3 direction) versus axial strains (left). All axial stresses are equal (Dillen, 2000).

et al., 1958). For the details of experimental set-up the reader is referred to Dillen (2000). We use the results of quasi-static and dynamic experiments where strains and ultrasonic compression waves were measured simultaneously for cubic rock samples of three different sandstones. The Flechtinger sandstone of the Upper Rotliegend Group, the Bad Dürckheim sandstone of the Lower Triassic age and the Niederhausen sandstone of the Rotliegend are analysed to establish a relation between the stress and the reflection coefficients under isotropic conditions. The geological and petrographical specifications of these sandstones can be found in Den Boer (1996), Den Boer et al. (1996), Den Boer and Fokkema (1996), Swinnen (1997) and Dillen (2000). Of interest here are the mass density, porosity and permeability, which are ρ=2.65, 2.66, 2.69 g/cm^3, ϕ=9%, 20%, 19% and k=0, 953, 2.6 mD for the Flechtinger, Bad Dürckheim and Niederhausen sandstones, respectively.

The quasi-static experiments are used to quantify the non-linear stress-strain relation as depicted in Fig. 1 under confining pressure conditions (all axial stresses equal) for the Flechtinger sandstone. In the generated stress versus strain curves, the assumed isotropy is partly destroyed by layer-induced transverse isotropic symmetry with respect to the vertical axis. The stress–strain relation is used to calculate static Young's Modulus (E) and the bulk compression modulus (K). Because of the non-linearity, a tangent modulus is calculated by finite differences after smoothing the data by a Gaussian function. The observed behaviour is in accordance with Walsh (1965).

On the other hand, the dynamic experiments are designed to measure the change in the propagating P- and S-wave velocities as a function of effective stress. P-wave velocities are measured in three propagation directions. S-wave velocities are measured in three propagation and polarization directions. An example of results from such experiments is shown in Fig. 2 for the Flechtinger sandstone under the same stress condition as in Fig. 1. As can be observed in the figure, both P- and S-wave velocities depend primarily on those axial stresses, which lie in the polarization and/or propagation direction. A common observation of the dynamic experiments carried out on different samples is that both P- and S-wave velocity changes become progressively smaller with increasing stress.

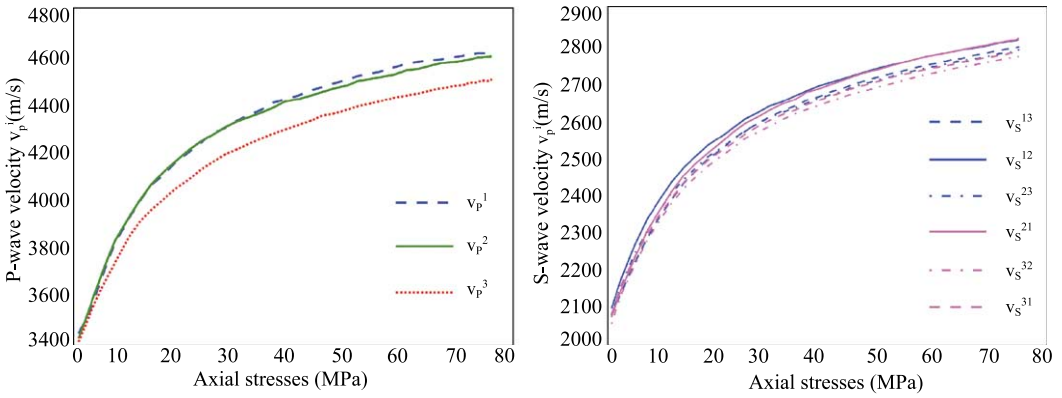

Fig. 2. Wave velocities as a function of uni-axial stress (τ_{33}), measured on a Flechtinger sandstone; P-wave velocity versus stress (left), S-wave velocity versus stress (right).

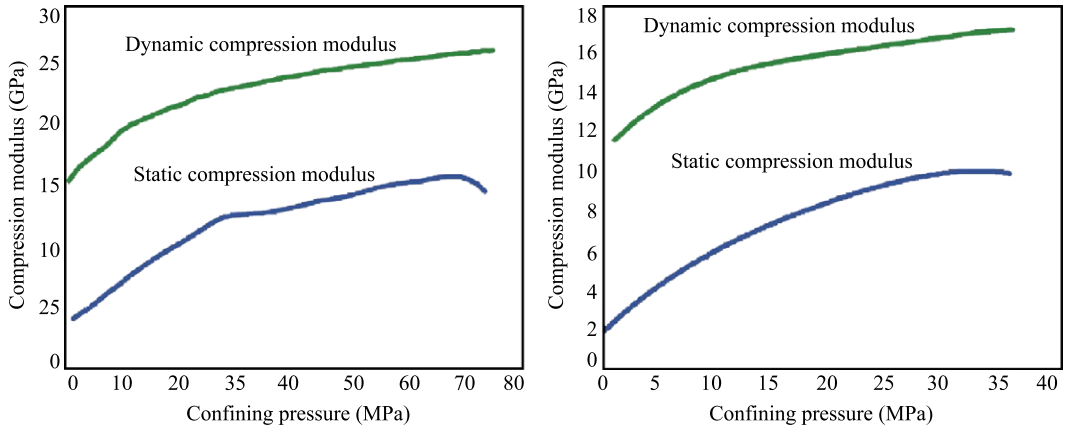

Fig. 3. The dynamic and static compression moduli for the Flechtinger sandstone (left), the Bad Dürckheim (right).

This observation generates an asymptotic behaviour in the velocity versus stress curves and postulates that near the asymptote all cracks are closed and the response to elastodynamic waves is close to the response that would be registered for the crack free or intact rock. From the velocity versus stress curves, dynamic material parameters are calculated. Fig. 3 shows the calculated static and dynamic bulk compression modulus. The dynamic compression modulus is larger than the static compression modulus over the entire stress range. The samples react stiffer to dynamic strains, and this behaviour supports the starting hypothesis. The rather large difference in static and dynamic behaviour may arise from the high frequencies at which the dynamic behaviour is determined; see Murphy (1984) for a discussion of the effects on crystalline rock. The central frequency of our ultrasonic experiments was 1 MHz.

Based on the static and dynamic elastic parameters calculated from the quasi-static and dynamic experiments, laterally homogeneous earth models consisting of two different layers are constructed for seismic modelling after upscaling. The reflection coefficients for vertical and oblique incidence were calculated. The calculations include PP reflections and converted PS waves. The converted waves depend primarily on the ratio of the shear velocities. For the calculation of reflection coefficients, the P-wave velocity propagating in the vertical axis (x_3) and the S-wave velocity propagating in the vertical axis (x_3) and polarized along the horizontal axis (x_1) are used. The S-wave velocity is influenced by both longitudinal and transverse stress changes. Evidence of this behaviour under for different loading stresses in different axial directions is not included here, but can be found in Dillen (2000).

The reflection coefficients are calculated for weak (<7%), medium (7–30%) and large (>30%) contrasts. The critical angles are calculated for all cases to determine an angle range for the sensitivity measurements of the reflection coefficients. Sensitivity analysis is carried out for pre-critical reflections.

The Poisson ratio is used to validate the approximations used in the calculation of reflection coefficients (Fig. 4). The dynamic Poisson ratio is calculated from the dynamic experiments. We first calculate the reflection coefficients by the Zoeppritz equations for PP and PS reflections and we invert for

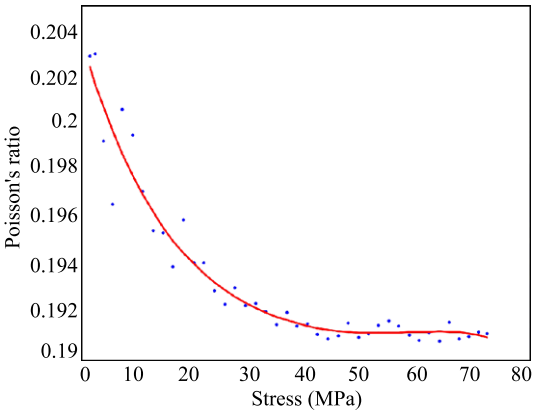

Fig. 4. The observed (dots) and fitted (solid line) dynamic Poisson's ratio versus stress for the Flechtinger sandstone.

the Poisson ratio using the linearized equations. Even for the weak contrast, the Poisson ratio calculated by the linearized inversion of reflection coefficients did not match the Poisson ratio calculated from the experimental results. Using linear approximations for this purpose requires a very small contrast between the layers. Impedance differences of 10% and 30% are not far from the real situations in nature. Therefore, it was decided to use the full Zoeppritz equations instead of the linearized equations. All angle-dependent reflection coefficients in this study are calculated by the full Zoeppritz equations.

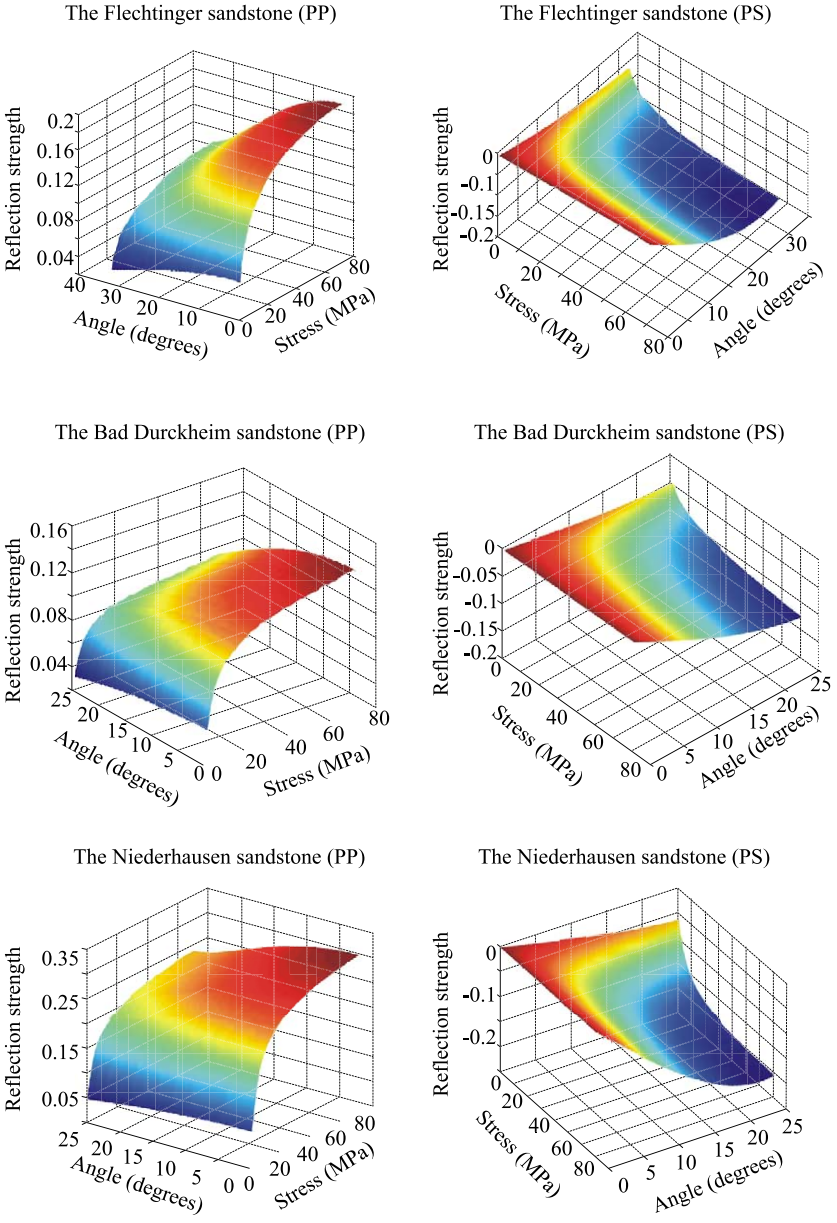

Fig. 5. PP (left) and PS (right) reflections as a function of angle and stress, medium to large contrast (as defined in Table 1) between two isotropic media for the three sandstones considered.

3. Angle-dependent reflection coefficients

To obtain an idea about the changes we can expect in the seismic reflection coefficients due to different stress levels near the interface between two different sand stones, some numerical experiments have been carried out to show the effect of stress in the dynamic elastic parameters for one of the two rocks at the interface. The assumption that the acoustic impedance depends on local stress condition for only the rock below the interface is not the most realistic situation, but it serves our purpose, as the relative changes in acoustic impedance will always change for changing stress conditions. This example should be interpreted as a study of the effect of different ratios that could exist under a certain range of stress conditions in the neighbourhood of an interface. For all three types of sandstone studied (Flechtinger, Bad Dürckheim and Niederhausen), Fig. 5 displays the angle-dependent reflection coefficients as a function of stress for medium contrasts, see Table 1 for the parameters used. Only the real part of the reflection coefficient is presented and will be named as "reflection strength" in the following paragraphs.

A remarkable increase of the reflection strength with increased stress is observed in PP reflections. The PP reflection is more sensitive to stress at the lower stress area, but there the angle dependency is weaker. The upward pattern of the PS reflection strength is due to approaching the critical angle. The PS reflection coefficient sensitivity to the effective stress is more homogeneous when lower and higher stress zones are compared. The PS reflection strength varies more regularly and systematically with the changing effective stress. This makes the PS reflection strength a more powerful tool to quantify the stress and reflection strength relation. However, the measured variation of the reflection strength at a fixed angle does not indicate a significant change at different stress ranges. The sensitivity of PS reflection strength to increasing effective stress is angle dependent, and can only be measured when the reflection strength is measured at different angles.

Table 1
Model parameters for the reflection coefficient computation of the Flechtinger, Bad Dürckheim and Niederhausen sandstones

	v_p (m/s)	v_s (m/s)	ρ (kg/m^3)
Layer 1	3200	1950	2500
Layer 2	3413–4501 Flechtinger sandstone	2083–2781 Flechtinger sandstone	2650 Flechtinger sandstone
	3194–4008 Bad Dürckheim sandstone	1923–2501 Bad Dürckheim sandstone	2660 Bad Dürckheim sandstone
Niederhausen sandstone			
Layer 1	3200	1950	2500
Layer 2	3413–4501	2083–2781	2650

4. From AVA to amplitude versus stress (AVS) analysis

From the above computed reflection coefficients, the intercept and gradient of the PP and PS reflections can be calculated (Dey-Sarkar and Svatek, 1993; Castagna and Smith, 1994) and a relation to stress can be established. Fig. 6 displays the amplitude versus angle information for the PP and PS reflections of three sandstone samples in the case of medium contrast The right-hand side of the figure displays the amplitude versus $\sin^2\theta$, where θ is the angle of incidence. For PP reflections, the curves with small amplitude values represent the lower stress zones, while for the PS reflections the higher curves represent the reflections at lower stress. The curves indicate that the angle dependency of the reflections increases with effective stress. The difference of the reflections at varying angles is less for the numerical measurements obtained under relatively lower effective stress. These phenomena are the same for PP and PS reflections. A common observation for both reflection coefficients, displayed in Fig. 6, is that they do not overlap at different angles. The angle-dependent PP and PS reflection coefficients are monotonic functions of stress.

The intercept and gradient are the usual parameters that are used in linear AVO or AVA analysis to quantify different material parameters through the relation with reflection coefficients (Aki and Richards, 1980; De Bruin, 1992). Although we do not use them to characterise our media, it is insightful to look at the values as a function of stress. The intercept represents the value of the reflection coefficient value for a plane wave at normal incidence. The gradient represents the first order derivative of the reflection coefficient with

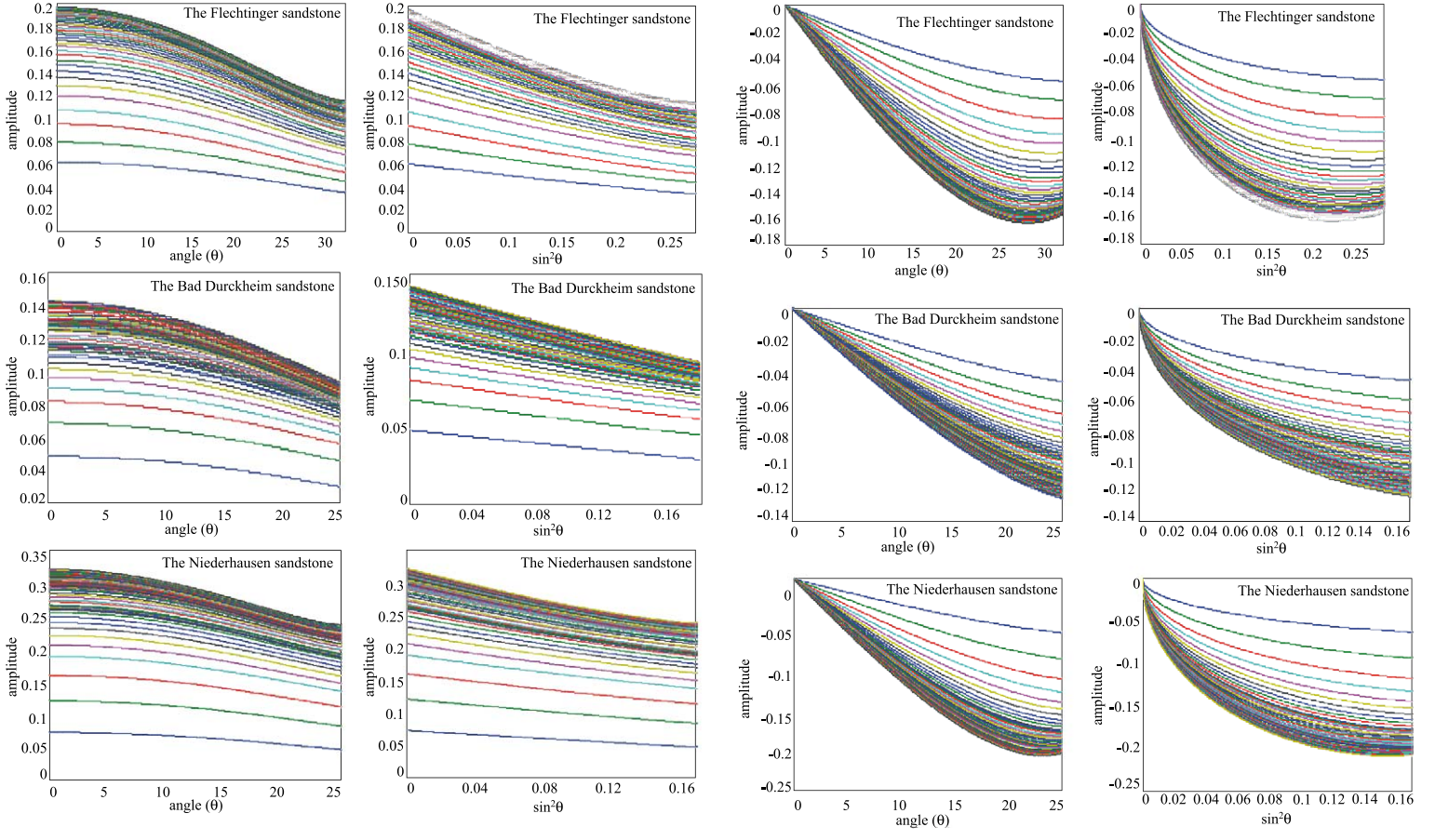

Fig. 6. Reflection strength versus angle (θ) and $\sin^2\theta$ of PP reflections (left) and PS reflections (right) for different stresses. The curves in the plots from small to large amplitudes correspond to increasing stress-values ranging from 0 to 80 MPa.

respect to angle. They are computed from the amplitude versus $\sin^2\theta$ curves by a linear regression analysis. Fig. 7 displays the gradient/intercept-stress relation for PP reflections of the Flechtinger, Bad Dürckheim and Niederhausen sandstones. The most interesting aspect of the plots is the absolute value of the gradient, which shows a remarkable increase with increasing effective stress for both PP and PS waves. Both intercept and gradient change more rapidly in the lower stress area up to 25 MPa. At higher stresses, they approach an asymptotic value and can be associated with the "crack model" (see Walsh, 1965). The irregularities in the curves of the Bad Dürckheim and Niederhausen sandstones are the results of different loops during the loading cycles in the experiments.

5. Optimisation techniques

The seismic data can provide input parameters of the geo-mechanical modelling after a realistic estima-

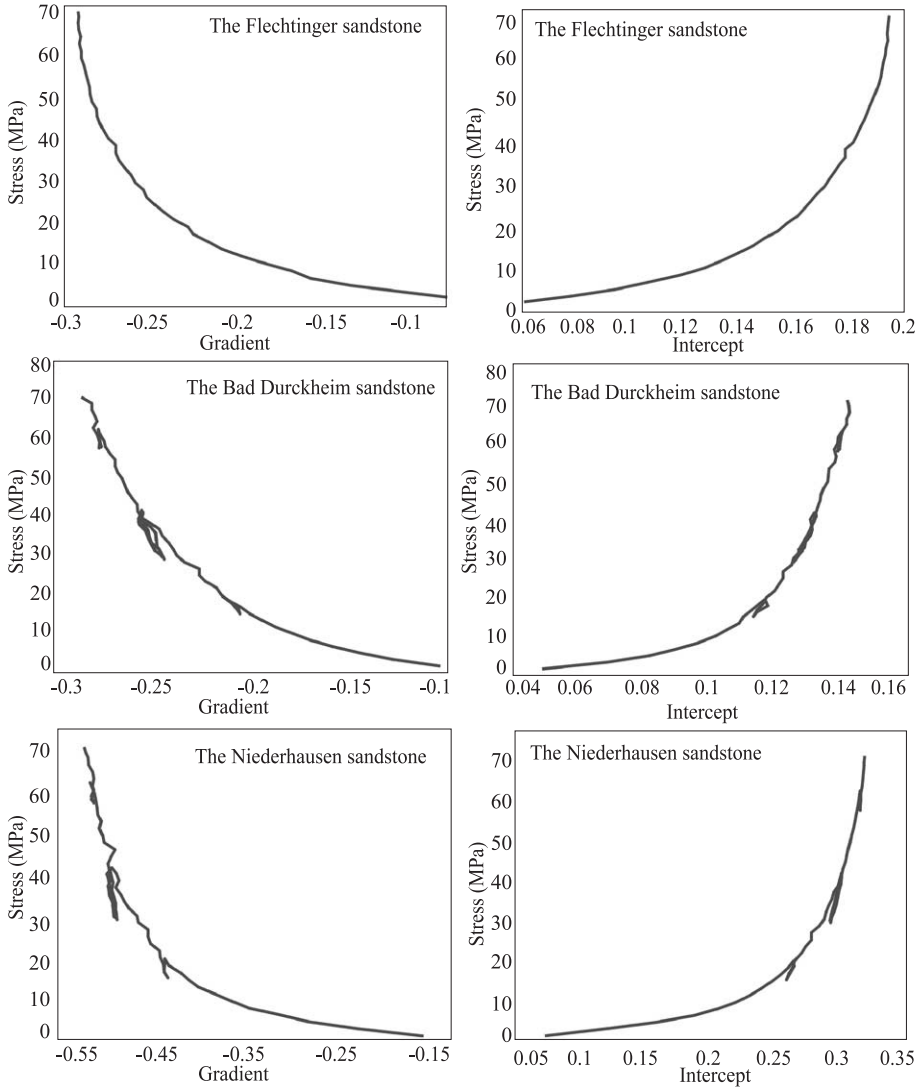

Fig. 7. Gradient (left) and intercept (right) of PP reflections for three different sandstones.

tion of the elastic material parameters. Estimation of the elastic material parameters requires an inversion of the reflection coefficients. The behaviour of different cost functions as a function of P-wave velocity (v_p), S-wave velocity (v_s) and density (ρ) were investigated prior to selecting any optimisation technique in combination with a cost function to be minimised, where a cost function can be defined as some kind of weighted difference between the data and the model. This is done by a quick global search, which uses simple function comparison methods to determine to what extent we can extract unknown parameters from the reflection coefficients. The results of global search prove that an accurate estimate of the unknown material parameters is possible by the inversion of reflection coefficients. Different cost functions with different norms (L_1, absolute error norm, and L_2, root mean square error norm) are constructed to investigate the capability and the sensitivity of PP and PS reflection coefficients separately as well as together for an inversion. Both single-angle and multi-angle cases are considered to measure the numerical stability and sensitivity of the optimisation techniques. Although in this study our models consist of only two isotropic layers, the method is applicable for any configuration.

All cost functions are optimised to minimise the difference between for three parameters (v_p, v_s, ρ). The direct search method with Nelder–Mead simplex algorithm (Nelder and Mead, 1965; Press et al., 1992) gave very accurate results for all three parameters. The Nelder–Mead simplex algorithm does not use numerical or analytic gradients. The search starts at an initial estimate and is also referred to unconstrained non-linear optimisation and has very good convergence properties for low number of unknowns and even for discontinuous cost functions (Lagarias et al., 1998).

5.1. Single angle inversion

The following cost function can be optimised when the measurements of the PP reflection coefficients at a fixed angle are used for the inversion:

$$C_p = \frac{\left|R^{pp}\left(\rho_2, v_{p2}, v_{s2}\right) - R^{pp}_{data}\right|}{\left|R^{pp}_{data}\right|} \tag{1}$$

where R^{pp} is the PP reflection coefficient and a function of velocity and density. We assume that the velocities and the bulk density of the first layer are known. With this assumption, we estimate the P-/S-wave velocities and the bulk density of the second layer while minimising this cost function. However, using PP reflection component as single component data alone without PS reflection component does not provide one single local minimum. Fig. 8 gives the cost function as functions of v_p-v_s, $v_p-\rho$ and $v_s-\rho$ and indicates that the cost function is not convex, when it is built by single-component data. As a result, there is no unique solution for the unknown elastic material parameters of the earth layers. In other words, it can be stated that the inversion of post-stacked single component data does not provide the elastic material parameters.

For non-zero angles, the following cost function can be optimised for the inversion of PP and PS reflection coefficients together:

$$C_1 = \frac{\left|R^{pp}\left(\rho, v_{p2}, v_{s2}\right) - R^{pp}_{data}\right|}{\left|R^{pp}_{data}\right|} + \frac{\left|R^{ps}\left(\rho, v_{p2}, v_{s2}\right) - R^{ps}_{data}\right|}{\left|R^{ps}_{data}\right|} \tag{2}$$

where R^{pp} and R^{ps} are the PP and PS reflection coefficients respectively and they are both measured at a fixed angle. This multi-component inversion provides more accurate results. Fig. 8 (right-hand side) displays the estimation of the P-/S-wave velocities and density after the optimisation of the cost function to be minimised.

The cost functions are also tested for the noisy data, generated by adding different percentages of noise to the seismic reflections. Comparison of the results from the noisy data shows that the cost functions are performing well even for the noisy data.

5.2. Multi-angle inversion

For multi-angle inversion of PP reflection coefficients, the following two cost functions can be optimised. The cost function with L_1 norm is:

$$C_1 = \frac{\sum_{\theta}\left|R^{pp}\left(\theta, \rho_2, v_{p2}, v_{s2}\right) - R^{pp}_{data}(\theta)\right|}{\sum_{\theta}\left|R^{pp}_{data}(\theta)\right|} \tag{3}$$

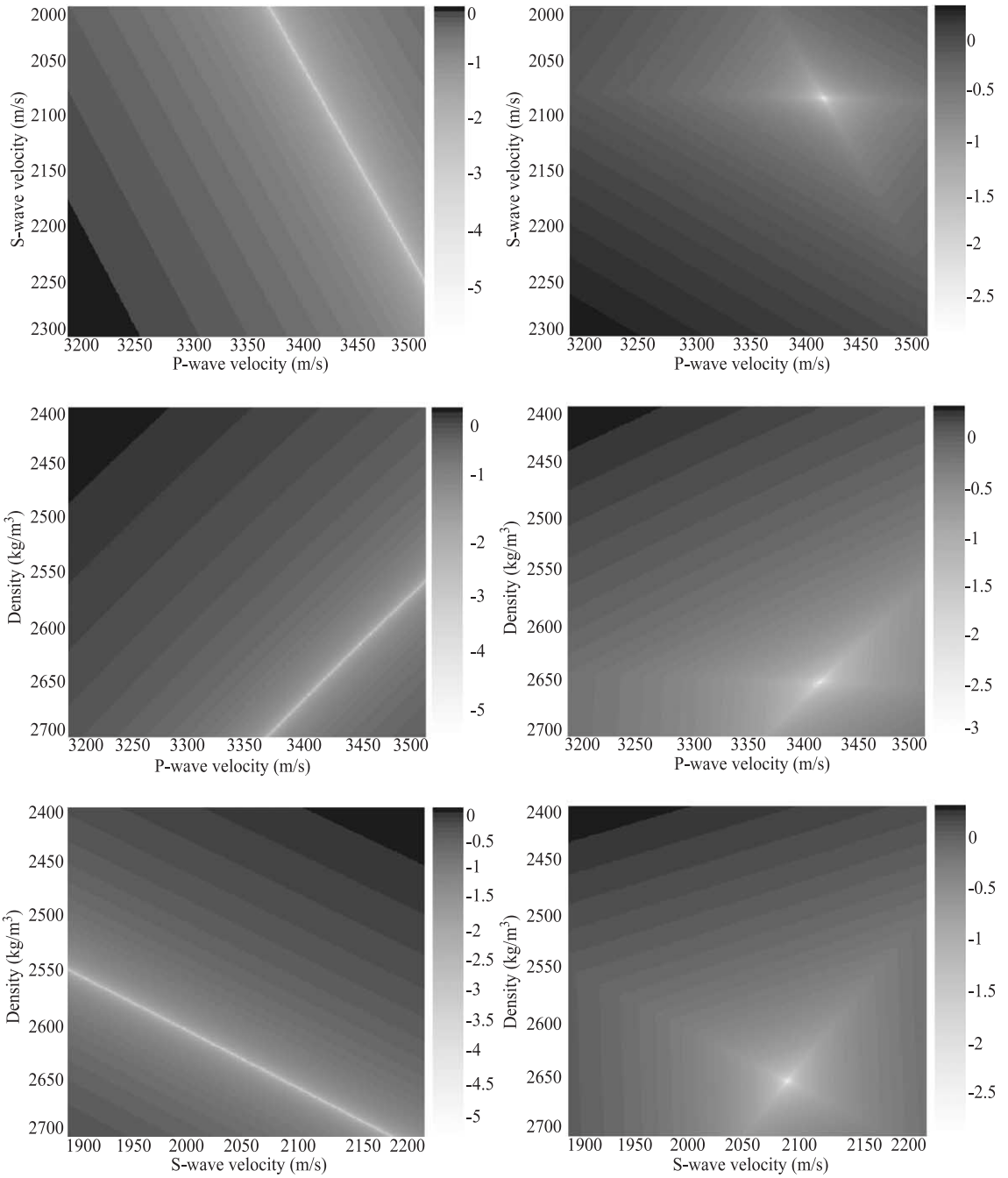

Fig. 8. Single angle optimisation of the "cost function with L_1 norm" including only PP reflections (left-hand side) and PP–PS reflections (right-hand side).

and the cost function with L_2 norm is:

$$C_2 = \frac{\left(\sum_{\theta} \left| R^{pp}\left(\theta, \rho_2, v_{p2}, v_{s2}\right) - R^{pp}_{data}(\theta) \right|^2 \right)^{1/2}}{\left(\sum_{\theta} \left| R^{pp}_{data}(\theta) \right|^2 \right)^{1/2}} \tag{4}$$

R^{pp} is the PP reflection coefficient and it is a function of P-wave and S-wave velocities, density and the angle. The cost function with L_2 norm is expected to be more precise, as it minimises the square of the difference between the estimated value and the real data. However, in case that the data are noisy, the cost function with L_1 norm may give better results because outliers receive less weight than in an L_2 norm.

The following two cost functions are optimised for multi-angle inversion of PP and PS reflection coefficients together. The cost function with L_1 norm is:

$$C_1 = \frac{\sum_{\theta} \left| R^{pp}\left(\theta, \rho_2, v_{p2}, v_{s2}\right) - R^{pp}_{data}(\theta) \right|}{\sum_{\theta} \left| R^{pp}_{data}(\theta) \right|} + \frac{\sum_{\theta} \left| R^{ps}\left(\theta, \rho_2, v_{p2}, v_{s2}\right) - R^{ps}_{data}(\theta) \right|}{\sum_{\theta} \left| R^{ps}_{data}(\theta) \right|} \tag{5}$$

The cost function with L_2 norm is:

$$C_2 = \frac{\left(\sum_{\theta} \left| R^{pp}\left(\theta, \rho_2, v_{p2}, v_{s2}\right) - R^{pp}_{data}(\theta) \right|^2 \right)^{1/2}}{\left(\sum_{\theta} \left| R^{pp}_{data}(\theta) \right|^2 \right)^{1/2}} + \frac{\left(\sum_{\theta} \left| R^{ps}\left(\theta, \rho_2, v_{p2}, v_{s2}\right) - R^{ps}_{data}(\theta) \right|^2 \right)^{1/2}}{\left(\sum_{\theta} \left| R^{ps}_{data}(\theta) \right|^2 \right)^{1/2}} \tag{6}$$

The optimisation results of the cost function with L_1 norm are displayed in Fig. 9. The left-hand side of the figure shows the stand-alone inversion of PP reflection coefficients. Although stand-alone inversion of PP reflection coefficients at a fixed angle does not provide one single local minimum, the multi-angle inversion of PP reflection coefficient without PS component provides one local minimum and unique solution to P- and S-wave velocities. This optimisation method can be used to extract earth parameters from the pre-stack single component seismic data. The right-hand side of the Fig. 9 displays the optimisation of the cost function with L_1 norm for the combined inversion of PP and PS reflections. The combined inversion of PP and PS reflections is the most stable tool to optimise the unknown elastic material parameters. A local minimum exists in all possible combinations. The solutions are more stable compared to the optimisation of the cost functions including both PP and PS reflection coefficients at a fixed angle. It also displays more accuracy than the multi-angle stand-alone inversion of PP reflection coefficient. This inversion can be used to obtain the elastic material parameters from the pre-stack multi-component real field data.

The cost functions for the multi-angle inversion were also tested for the data containing up to 50% noise. The results show that multi-angle, multi component and multi-angle single component inversion of the noisy data is possible by the cost functions described in Eqs. (3)–(6). The cost functions with L_1 and L_2 norms both perform efficiently to solve the inversion of noisy seismic reflections.

6. Conclusions

A methodology is developed to relate the offset-dependent seismic reflections to the local stress distributions. Our working hypothesis, that the static and dynamic elastic parameters are related through the static state of stress, is validated by physical experiments on three different types of sandstones. Reliable local stress distributions can be computed only when accurate dynamic elastic material parameters are obtained from inversion of seismic reflections. To accurately determine the dynamic elastic parameters from seismic reflection coefficients, the full Zoeppritz equations are essential to be used in parametric inversion. The direct comparison of the PP and PS reflections shows that they are both very sensitive to stress. The sensitivity decreases as the stress increases, while the angle dependency increases with increasing stress, making pre-stack analysis more important at higher stress levels. The sensitivity of PS reflections

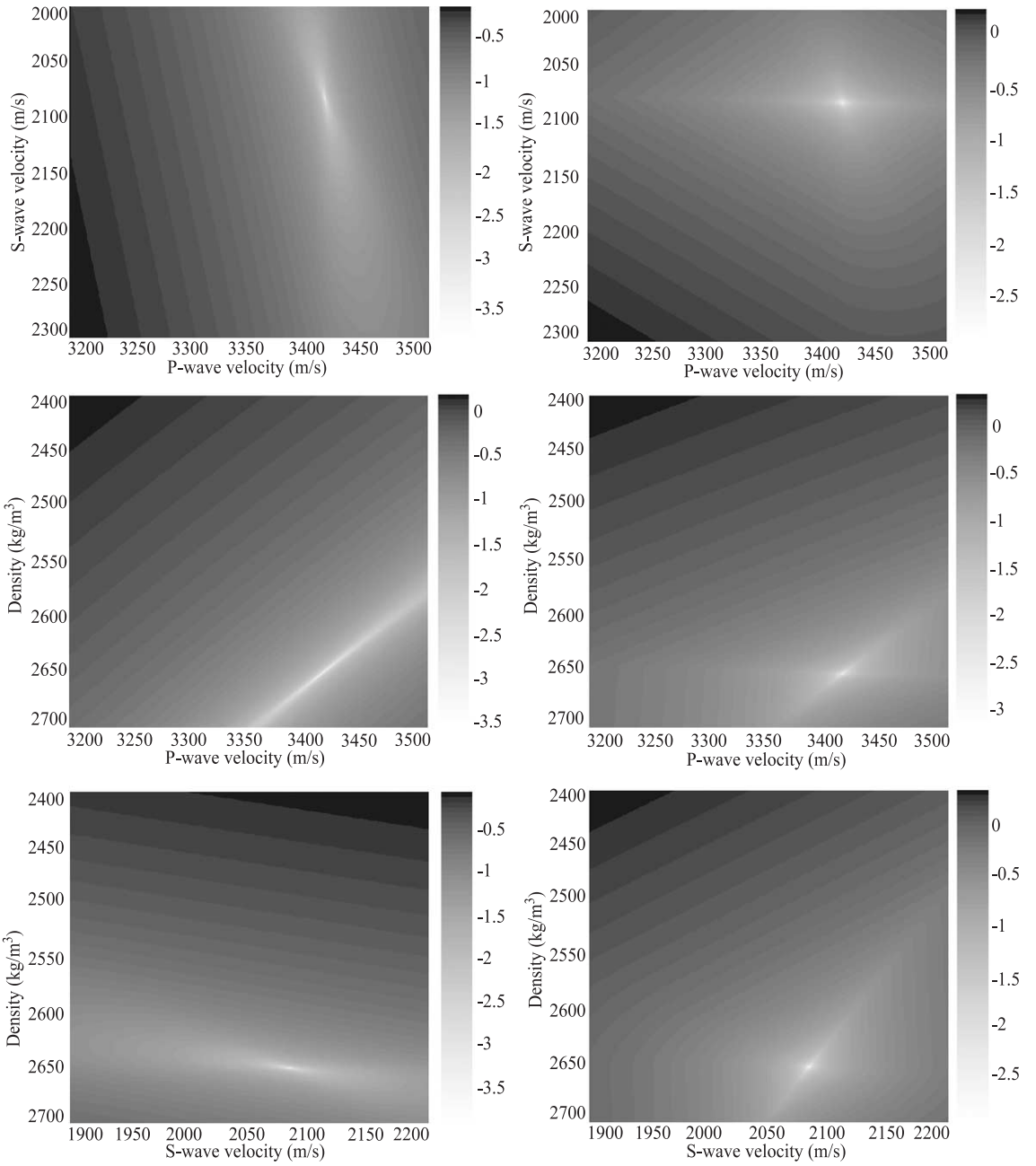

Fig. 9. Multi-angle optimisation of the "cost function with L_1 norm" including only PP reflections (left-hand side) and PP–PS reflections (right-hand side).

can be determined accurately when the reflection coefficients are obtained as a function of the incident angle. The regular pattern of the changes in PS reflections makes the pre-stack PS reflection analysis more powerful to quantify the relation of seismic reflections and stress.

The inversion of PP and PS reflections together provides unique solutions to the dynamic elastic

parameters. From the obtained dynamic material parameters, the static parameters follow when their relation is known, either from measurements, as we have shown, or from a rock-physics model. In that case, these derived static parameters are used as input in geo-mechanical modelling to compute the static state of stress in the upper crust at different scales. This is, of course, under the assumption that good estimates of the regional tectonic forces are known. This will improve the accuracy of the geo-mechanical modelling.

Acknowledgment

The Netherlands Research Centre for Integrated Solid Earth Science (ISES) financially supports this work, which is gratefully acknowledged.

References

Aki, K., Richards, P., 1980. Quantitative Seismology—Theory and Methods. W.H. Freeman, San Francisco.

Beekman, 1994. Tectonic modelling of thick-skinned compressional intraplate deformation. PhD thesis, Vrije Universiteit-Amsterdam, p. 152.

Castagna, J.P., Smith, S.W., 1994. Comparison of AVO indicators: a modelling study. Geophysics 59, 1849–1855.

Castagna, J.P., Batzle, M.L., Kan, T.K., 1993. Rock physics: the link between rock properties and AVO response. In: Castagna, J.P., Backus, M.M. (Eds.), Offset-Dependent Reflectivity—Theory and Practice of AVO Analysis. SEG, Tulsa, pp. 135–171.

Cheng, C.H., Johnston, D.H., 1981. Dynamic and static moduli. Geophys. Res. Lett. 8, 39–42.

De Bruin, C., 1992. Linear AVO inversion by prestack depth migration—imaging angle dependent reflectivity as a tool for litho-startigraphic inversion. PhD thesis, Delft University of Technology. 220 pp.

Den Boer, E.G., 1996. The effect of stress on wave propagation in Aeolian Rotliegend sandstone. MSc thesis, Delft University of Technology, Department of Applied Earth sciences. MP/TG 1996-01.

Den Boer, E.G., Fokkema, J.T., 1996. Scaling propagation phenomena as result of externally applied isotropic stress on an Aeolian Rotliegend sandstone sample. Society of Exploration Geophysicists (SEG) International Exposition and 66th Annual Meeting, Expanded Abstracts, vol. 2. Denver, Colorado, pp. 1703–1706.

Den Boer, E.G., Dillen, M.W.P., Duijndam, A.J.W., Fokkema, J.T., 1996. The effect of stress on wave propagation in Aeolian Rotliegend sandstone. European Association of Geoscientists and Engineers (EAGE) 58th Conference and Technical Exhibition, Extended Abstracts, vol. 1. P071, Amsterdam, The Netherlands.

Dey-Sarkar, S.K., Svatek, S.V., 1993. Prestack analysis—an integrated approach for seismic interpretation in clastic basins. In: Castagna, J.P., Backus, M.M. (Eds.), Offset-Dependent Reflectivity—Theory and Practice of AVO Analysis. SEG, Tulsa.

Dillen, M.W.P., 2000. Time-lapse seismic monitoring of subsurface dynamics. PhD thesis, Delft University of Technology, Department of Applied Earth Sciences, ISBN 9014406-4.

Lagarias, J.C., Redes, J.A., Wright, M.H., Wright, P.E., 1998. Convergence properties of the Nelder–Mead simplex algorithm in low dimensions. SIAM J. Optim. 9, 112–147.

Landrø, M., Digranes, P., Strønen, L.K., 2001. Mapping reservoir pressure and saturation changes using seismic methods—possibilities and limitations. First Break 19, 671–677.

Linjordet, A., Skarpness, O., 1992. Application of horizontal stress directions interpreted from borehole breakouts recorded by four-arm calliper dipmeter tools. In: Vorren, T.O., Bersager, E., Dahl-Stammes, Ø.A., Holter, E., Johansen, B., Lie, E., Lund, T.B. (Eds.), Arctic Geology and Petroleum Potentials. Elsevier, Amsterdam, pp. 681–690.

Murphy III, W.F., 1984. Seismic to ultrasonic velocity drift: intrinsic absorption and dispersion in crystalline rock. Geophys. Res. Lett. 11 (12), 1239–1242.

Nelder, J.A., Mead, R., 1965. A simplex method for function minimization. Comput. J. 7, 308–313.

Plona, T.J., Cook, J.M., 1995. Effects of stress cycles on static and dynamic Young's moduli in Castlegate sandstone. In: Daemen&Schults (Ed.), Rock Mechanics. Balkema, Rotterdam, pp. 155–158.

Press, W.H., Teukolsky, S.A., Vetterling, W.T., Flannery, B.P., 1992. Numerical Recipes in Fortran, the Art of Scientific Computing, 2nd ed. Cambridge University Press, Cambridge. 963 pp.

Simmons, G., Brace, W.F., 1965. Comparison of static and dynamic measurements of compressibility of rocks. J. Geophys. Res. 70, 5649–5656.

Swinnen, G., 1997. The effect of stress on wave propagation in reservoir rocks. MSc thesis, Katholieke Universiteit Leeuwen, Department of Civil Engineering.

Van Balen, R.T., Cloetingh, S., 1993. Intraplate stresses and fluid flow in extensional basins. In: Horbury, A., Robinson, A. (Eds.), Diagenesis and Basin Development, Am. Assoc. Pet. Geol. Stud. Geol., 34, pp. 87–98.

Van Balen, R.T., Cloetingh, S., 1995. Neural network analyses of stress induced overpressures in the Pannonian Basin. Geophys. J. Int. 121, 532–544.

Walsh, J.B., 1965. The effects of cracks on the compressibility of rock. J. Geophys. Res. 70 (2), 381–389.

Wyllie, M.R.J., Gregory, A.R., Gardner, L.W., 1958. An experimental investigation of factors affecting elastic wave velocities in porous media. Geophysics (23), 459–493.